Heliyon 9 (2023) e15462

Contents lists available at ScienceDirect

Heliyon

journal homepage: www.cell.com/heliyon

Research article

Investigations on the microstructure and properties of yttria and silicon carbide reinforced aluminium composites

P.P. Shantharaman [a], V. Anandakrishnan [b], S. Sathish [c], M. Ravichandran [d,*], R. Naveenkumar [d], S. Jayasathyakawin [d], S. Rajesh [e]

[a] Department of Mechanical Engineering, Kings College of Engineering, Punalkulam, 613303, Tamil Nadu, India
[b] Department of Production Engineering, National Institute of Technology, Tiruchirappalli, 620 015, Tamil Nadu, India
[c] Department of Mechatronics Engineering, K.S. Rangasamy College of Technology, Tiruchengode, Namakkal, 637215, Tamil Nadu, India
[d] Department of Mechanical Engineering, K Ramakrishnan College of Engineering, Samayapuram, 621112, Trichy, Tamil Nadu, India
[e] Department of Mechanical Engineering, Kalasalingam Academy of Research and Education, Krishnankoil, 626126, Virudhunagar, Tamil Nadu, India

A R T I C L E I N F O

Keywords:
Aluminium
Composites
Silicon carbide
Powder metallurgy
Properties

A B S T R A C T

Powder Metallurgy (PM) was used to synthesize SiC (0, 5, 10, 15 & 20 wt%) and 1 wt% Yttria (Y_2O_3) reinforced aluminium (Al) metal matrix composites. The Al–SiC–Y_2O_3 hybrid composites samples were prepared for density (ρ), hardness (VHN), mechanical, tribological, and micro-structural studies in accordance with ASTM standards. SEM images revealed an even spreading of SiC particles throughout the Al matrix and composition was verified by the characterization techniques. The addition of SiC and Y_2O_3 to their respective composites improved the VHN and 'ρ'. The compressive strength (CS) of Al–SiC–Y_2O_3 composites increased while increasing the SiC. The higher compression strength (405 MPa) was obtained for the Al − 1 wt% Y_2O_3-20 wt% SiC-hybrid composites. The thermal conductivity (K) of Al–SiC–Y_2O_3 samples diminishes, as the hard SiC particles are gradually added. Furthermore, it was observed that accumulative the wt% of SiC in the aluminium metal matrix (AMMC) results in a novel material with a decreased wear rate. The better properties was achieved for the samples contain 20 wt% of SiC content in Al − 1 wt% Y_2O_3 matrix.

1. Introduction

Metal matrix composites (MMCs) have established an excessive deal of consideration in last few decades due to their outstanding features that combine the best of matrix phase and reinforcing qualities [1–4]. In general, the best matrix materials are ductile metal alloys, while the best reinforcement particles are hard ceramics. Aluminium, copper, titanium and magnesium are some of the commonly researched matrix materials [5,6]. Aluminium (Al) is the most favoured matrix material among these materials due to its extraordinary properties. Modern reinforcing ceramic materials have a wide range of applications in mechanical, electrical, electronics, aeronautic, automobile, and chemical engineering, among others, due to their exceptional physical and mechanical qualities and characteristics. In recent years, Al matrix composites have become increasingly popular for military and automotive applications due to its superior properties [7].

* Corresponding author.
E-mail address: ravichandran@krce.ac.in (M. Ravichandran).

https://doi.org/10.1016/j.heliyon.2023.e15462
Received 4 November 2022; Received in revised form 30 March 2023; Accepted 10 April 2023
Available online 12 April 2023

Unfortunately, the inherent brittleness of ceramic materials continues to be a significant setback. Researchers attempted to reduce the brittleness of ceramic materials, as well as to alter the flexural strength and fracture toughness, with some success. Rare earth elements, on the other hand, have found broad use in a variety of ceramics as useful additions due to their unique properties. It is indeed one of the most significant topics in ceramic composites research right now. Generally, $A1_2O_3$, TiC, SiC, TiB_2, Si_3N_4, sialon, and A1N ceramics are utilised as reinforcements. Rare earth yttrium can be used as reinforcement to increase mechanical properties [8–10]. Many researchers recommended PM is the best process over liquid processing routes [11–13]. Navdeep Singh et al. investigated tribological study of Al/SiC based composite that was made via PM and conducted ANOVA test to identify % contribution of various parameters related to wear properties [14]. Reza Zare et al. explored the impact of volume percent of SiC particle on the properties of Al (6061) matrix composite [15]. The PM approach was used by Negin Ashrafi et al. to fabricate the hybrid Fe_3O_4–SiC incorporated new composite and they concluded that the addition of Fe_3O_4 and SiC to the (AMMC) increased the magnetic property and the thermal characteristics.

A hybrid composite has specific merits over conventional composites, including good strength, reduced weight and improved fatigue resistance [16]. Several studies have described on the wear performance of hybrid Al composites at the micro level. Furthermore, there is a scarcity of literature on Al–SiC–Y_2O_3 hybrid composites. As a result, SiC and Y_2O_3 particles were used as a secondary particles for the Al matrix in this study. The goal of this work is to use mechanical milling and powder metallurgy techniques to develop hybrid Al/SiC/Y_2O_3 composites to inspect the mechanical and wear performance of the composite. SEM examination was used to examine the microstructures of the composites. Density, hardness, and compression tests were used to conclude mechanical parameters.

2. Experimental setup and procedures

Al was employed as the basic material in the current experimental work (provided by The Metal Powder Company Ltd., Madurai). Average sizes of the matrix powder was 30 μm. The reinforcing materials were commercially available SiC particles of average sizes of 100 μm and Y_2O_3 particles of average sizes of 50 nm. Ball milling process was used to obtain consistent particle dispersion. Powders were weighed using an electronic weighing equipment with a 0.001 g accuracy level and uniformly blended using a planetary mixer with carbide balls. The diameter of ball were 12 mm. To obtain the Al/SiC/Y_2O_3 composite powders, 5, 10, 15, 20 wt% SiC and 1 wt% Y_2O_3 were introduced to the Al matrix material. The ball to powder weight ratio of 10:1 was employed to mill the powder for up to 3 h. In a uniaxial press, powders were cold compressed to prepare samples with a dimensions of 12*24 mm. Fig. 1 shows the punch and die used for the compaction process. Graphite particles were used to manually lubricate the die wall for each run [7]. Green compacts were sintered for 2 h at 600 °C in an electric muffle furnace.

Conventional process was used to polish the produced sample to conduct the microstructure and compositional studies. Initially, the samples were rough polished using typical abrasive sheets of 400, 1000, 1400, and 2200 grits. After that, the composite preforms were fine polished with a size of 1-μm diamond paste. For improved microstructural images, Keller's reagent was used as etchant. X-Ray Diffraction analysis (XRD) were analyzed for the sintered composites with a Cukα (λ = 1.54060 A°).

The theoretical and experimental densities of Al hybrid composites with varied wt% SiC and constant 1 wt% Y_2O_3 were analyzed. The theoretical 'ρ' was measured by considering the density of Al, SiC and Y_2O_3 (2.7, 3.21 and 5.01 g/cm^3, respectively) using standard equation (1) according to the composition.

$$Theoretical\ Density = \frac{100}{\frac{Density\ of\ Matrix}{Weight\ Percentage} + \frac{Density\ of\ Reinforcment}{Weight\ Percentage}} \tag{1}$$

The Archimedes principle was used to measure the experimental 'ρ' of specimens, [17,18]. The experimental 'ρ' was calculated by using this equation (2) and weighing balance was used to achieve the weight of each proposed specimens.

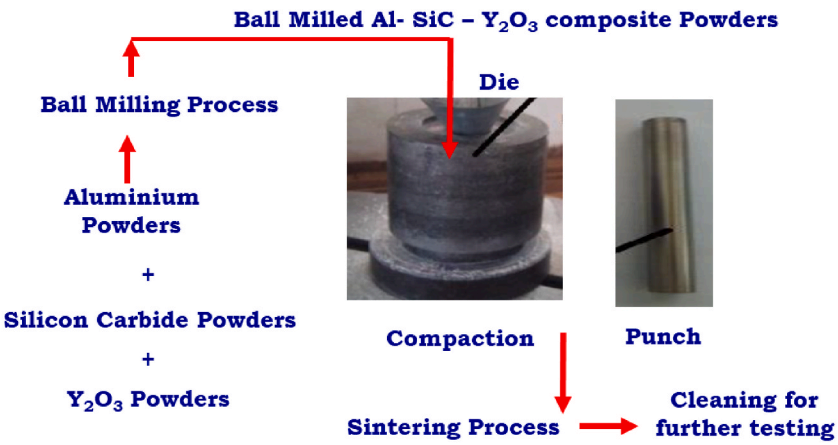

Fig. 1. Punch and die used for preparing the samples.

$$Experimental\ Density = \frac{Weight\ of\ the\ sample\ in\ Air}{Weight\ of\ the\ sample\ in\ air - weight\ of\ the\ sample\ in\ Water} X\ Density\ of\ Water \tag{2}$$

The porosity of the specimens was measured by using equation (3).

$$Porosity = \frac{Theoretical\ Density\ of\ the\ sample - Experimental\ Density\ of\ the\ sample}{Theoretical\ Density\ of\ the\ sample} X\ 100 \tag{3}$$

Vickers hardness tester according was done as per ASTM E 92 standard. After polishing with fine grained emery sheets, Vickers hardness test was conducted on the composite samples. A weight of 0.3 kg was applied with a stay time of 15 s. The average of five different test locations of the samples was taken as the hardness value. The Al–SiC–Y_2O_3 composites were tested for CS in an Instron test machine at room temperature [19,20]. The tests had been carried out at a constant strain rate. K was evaluated using K measurement apparatus to study the effect of reinforcements on the sintered composites [21]. ASTM G 99 was followed to conduct the wear test on a pin-on-disk. The pins were made of sintered hybrid composite materials and tested by sliding them on a steel disc (EN31 steel). Prior to each test, the specimens and the steel disc were ground with emery paper on their surfaces. Running-in-wear was applied to the specimens with a weight of 3 kg and a sliding speed of 250 rpm. Before and after each test, the materials were prepared with acetone and weighed with an electronic balance with a resolution of 0.001 mg [22]. The wear rate was calculated by using the below equation (4). The COF values were calculated by dividing the frictional force with applied load. The worn surfaces and microstructure of the composite specimens were analyzed by SEM (Make: TESCAN VEGA3-Wsource).

$$Wear\ Rate = \frac{Volume\ Loss\ (mm^3)}{Sliding\ Distance\ (m)} \tag{4}$$

3. Results and discussions

3.1. Microstructural characterization

The spreading of the reinforcement is the most major factor in achieving consistent characteristic of discontinuously reinforced composite materials. The microstructure provides insight into the composites performance. The SEM micrographs of the sintered composite materials demonstrate consistent SiC and Y_2O_3 particle distributions in the Al matrix. Fig. 2(a) shows the morphology of Al + 1 wt% Y_2O_3 + 5 wt% SiC composite. Fig. 2(b) displays the morphology of Al + 1 wt% Y_2O_3 + 10 wt% SiC composite. Uniform distribution was observed for the both samples. Fig. 2(c) displays the morphology of Al + 1 wt% Y_2O_3 + 15 wt% SiC composites. Fig. 2

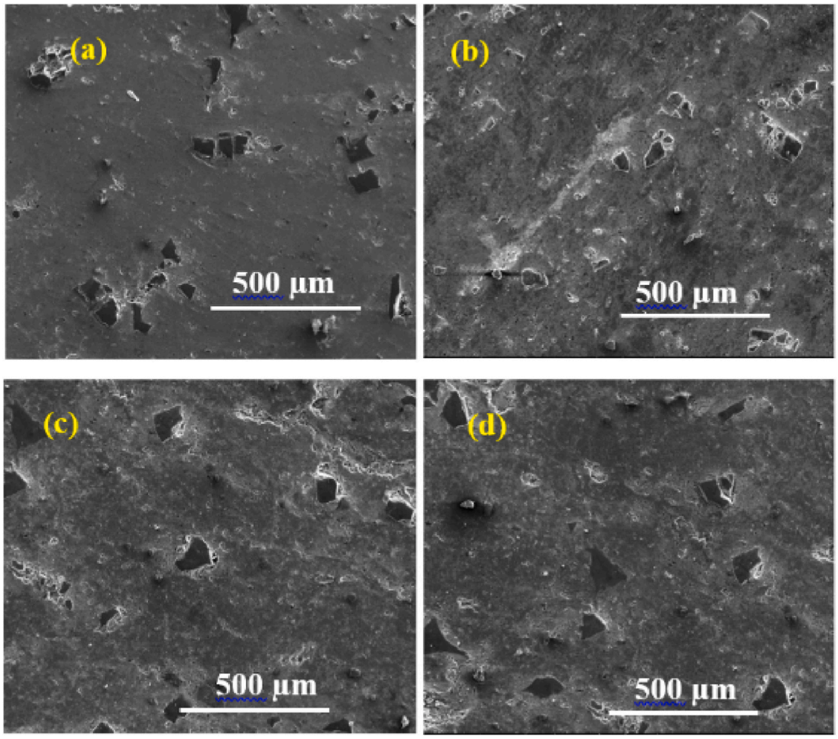

Fig. 2. SEM images (a) Al + 1 wt% Y_2O_3 + 5 wt% SiC, (b) Al + 1 wt% Y_2O_3 + 10 wt% SiC, (c) Al + 1 wt% Y_2O_3 + 15 wt% SiC and (d) Al + 1 wt% Y_2O_3 + 20 wt% SiC.

(d) displays the morphology of Al + 1 wt% Y_2O_3 + 20 wt% SiC composites. Higher reinforcement intensity is seen in composites with 15 and 20 wt% SiC. The presence of these high amount of SiC appears to be the cause of the porosity. The connection between the particles in matrix is weak when the porosity is high.

Fig. 3 displays the XRD pattern for the Al − 20 wt% SiC- 1 wt% Y_2O_3 composites. Al is the foremost peak and it indicates the no impurities were formed during furnace heating. SiC peak is seen the composite samples evident the strength improvement. Y_2O_3 peak is not seen in the pattern because of presence of less wt% (1 wt%). Fig. 4 shows the EDAX of Al − 20 wt% SiC-1 wt% Y_2O_3 composites. Al peak is observable from the plot and it displays the relevant SiC and Y_2O_3 peaks.

3.2. Density and porosity

Fig. 5 clearly shows that, the theoretical densities of the sintered specimens are superior than experimental densities. Both the theoretical and experimental 'ρ' values are improved for the rise in wt% of SiC particles. The experimental density values of the Al–SiC–Y_2O_3 composites increased linearly, as shown in Fig. 5. The higher 'ρ' of SiC particles compared to unreinforced Al particles accounts for the increase in composite 'ρ'. As was shown in Fig. 5, the 'ρ' of the sintered specimens increased as the SiC content increased. Increase in SiC wt% increases the porosity of the samples. Increase in porosity decreases the 'ρ' of the samples [17]. Because of the presence of pores and voids, there is always a disparity between theoretical and experimental 'ρ' values. Pores also have a noteworthy influence on the composite material's mechanical properties and it assist as pre-existing fracture sites where crack origination and propagation can take place. As a result, understanding voids is critical for improving composite quality [18]. Fig. 6 depicts the relationship between porosity and reinforcement content of Al–Y_2O_3–SiC hybrid composites. The porosity levels was found to be increased with rise in SiC content.

3.3. Mechanical characterization

The average VHN of the Al–Y_2O_3–SiC composites is revealed in Fig. 7. Increasing the wt% of SiC in the AMMC increases the VHN of hybrid composites. The addition of reinforcing particles boosts the composite's hardness form 92 VHN to 143 VHN. The high stiffness of SiC particles and the robust interfacial interaction between Al and SiC are the reasons for the composite's increased VHN. Furthermore, the ceramic SiC and yttria particles slowed the effort of dislocations, limiting the deformation of the composite and accounting for the increased VHN.

Fig. 8 depicts the composites' CS as a role of the adding of SiC particles. Al − 1 wt% Y_2O_3-20 wt% SiC composite exhibited the maximum CS as 405 MPa. According to Fig. 8, the CS of the Al–Y_2O_3–SiC composites follows linear increase with increase in weight percent of SiC reinforcement particles. Due to its hard and strong nature, SiC plays a crucial part in strengthening the composite material's and load-bearing capability [19]. Also, the bonding that are responsible for the considerable development in CS properties of Al–Y_2O_3–SiC composites and even dissemination of reinforcing particles in the matrix [20]. Compressive and tensile strengths of Al composites could be greatly improved by including the reinforcements like silicon carbide [23].

3.4. Thermal conductivity

The influence of SiC and Y_2O_3 particle additions on the K of hybrid composites is shown in Fig. 9. K is reduced when SiC is added to the Al matrix. When larger weight percentages of SiC particles are added to the Al–Y_2O_3–SiC composite, the K drops. In general, K of is inclined by the kind of reinforcement, particles grade, wt%, densities or porosities, and the processing technique utilised [21]. With the

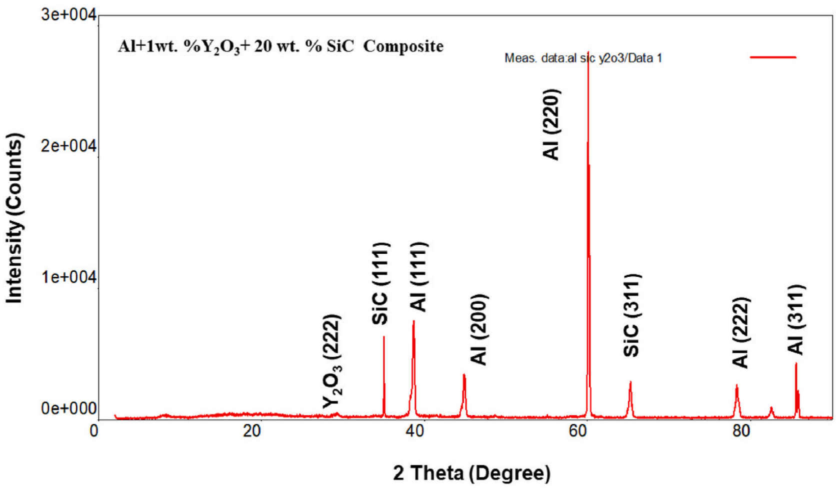

Fig. 3. XRD pattern Al–SiC–Y_2O_3 hybrid composites.

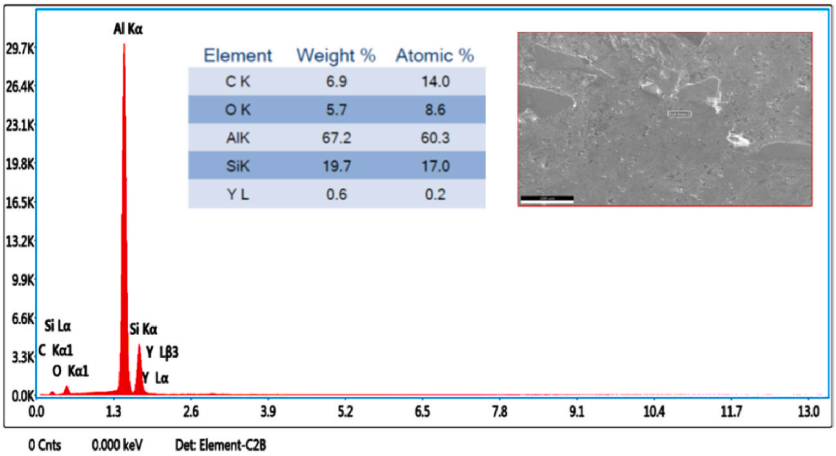

Fig. 4. EDAX of Al–SiC–Y_2O_3 hybrid composites.

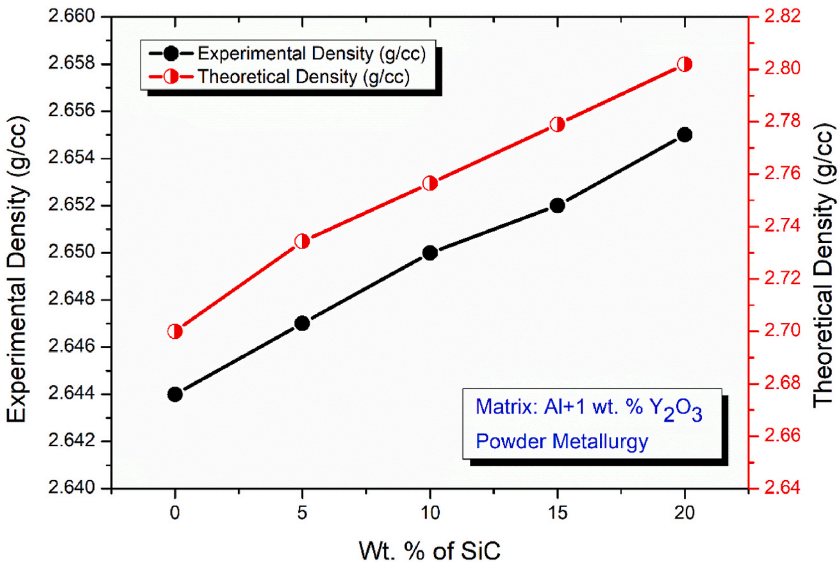

Fig. 5. Density of Al + 1 wt%Y_2O_3 + SiC hybrid composites.

inclusion of SiC and Y_2O_3 reinforcements, K decreases from 192 to 118 W/k. With the addition of SiC and Y_2O_3 particles to Al, the interfacial area and interfacial thermal resistance grow, resulting in a drop in K. Also, the porosity of Al–Y_2O_3–SiC composites also affects its K in a complex way. The pores might be considered a scattered phase, and hence the increased porosity lowers the heat conductivity.

3.5. Wear analysis

Fig. 10 shows the wear analysis findings of Al–Y_2O_3–SiC hybrid composites produced. Fig. 10 explicitly describes that as compared to Al metal, AMMC with SiC have lower wear rates, and the wear rate falls dramatically as the amount of SiC particle reinforcements in composite materials increases. For example, the wear rate for Al with 20 wt% SiC is 0.00626 mm^3/mm whereas the wear rate of Al is 0.00716 mm^3/mm. The enhancement in wear resistance of hybrid composites with higher reinforcing content is due to the composite's increased VHN. The friction coefficients at various SiC wt% are display in Fig. 11. As can be seen in the graph, raising the SiC weight percentage in the matrix decreases the COF and less than the pure Al. In addition to the SiC content the existence of Y_2O_3 also pay to the wear properties of the Al–Y_2O_3–SiC composites. This is confirmed by the previous study which explains that, the accumulation of Y_2O_3 can improve the internal structure and can increase the wear properties [22]. For the matrix material, the adhesive wear was observed owing to the accounting of plastic deformation when the pin contacted the disc with load. However, the abrasive wear was observed for the composite samples due to the occurrence of SiC and Y_2O_3 in the ductile matrix.

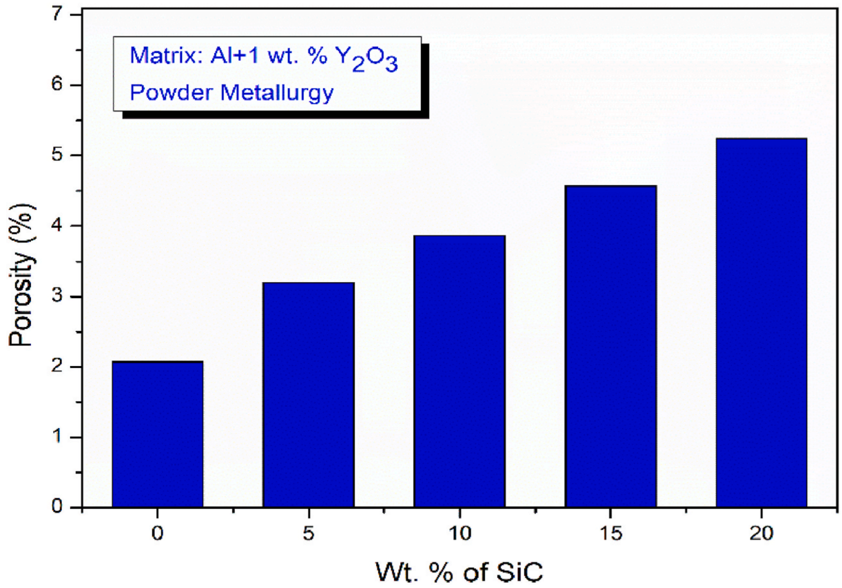

Fig. 6. Porosity of Al + 1 wt%Y_2O_3 + SiC hybrid composites.

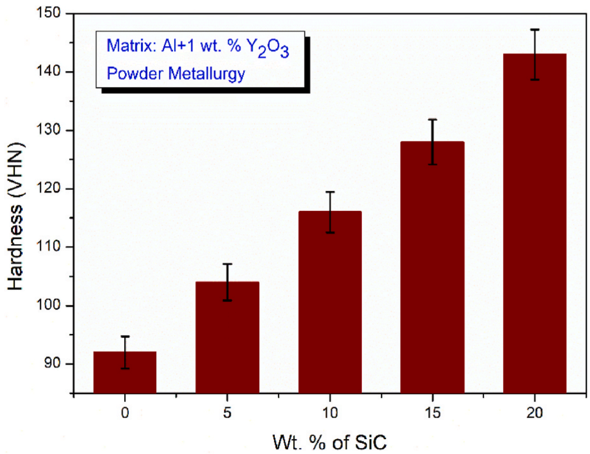

Fig. 7. Hardness of Al + 1 wt%Y_2O_3 + SiC hybrid composites.

3.6. Worn surface analysis

Fig. 12(a)–(d) shows the SEM images of the worn surfaces of the Al–Y_2O_3–SiC hybrid composites samples. Fig. 12(a) show the worn surface of the Al + 1 wt% Y_2O_3 + 5 wt% SiC composite. It displays the development of deep plough and fine scratches on the surface of the wear track, which recommended abrasive wear in the samples. Fig. 12(b) show the worn surface of the Al + 1 wt% Y_2O_3 + 10 wt% SiC composite. It shows the development of plough, scratches, deformed layers and craters on the surface of the wear track, which recommended abrasive wear, adhesive wear and delamination in the worn samples. In addition the surface cracks are observed in the worn surface which may further lead to crater. Fig. 12(c) show the worn surface of the Al + 1 wt% Y_2O_3 + 15 wt% SiC composite. It shows the development of scratches, plough, deformed layers and fine powder debris on the surface of the wear track, which recommended abrasive wear, adhesive wear and oxidation wear in the samples. Fig. 12(d) show the worn surface of the Al + 1 wt% Y_2O_3 + 20 wt% SiC composite. It shows the development of plough, scratches, and craters with the fine oxidized powders on the surface of the wear track, which recommended abrasive wear, and delamination in the worn samples. The formation of oxide layers acted as the surface lubrication which helps in the increased wear resistance. Due to the presence of SiC particles, the shrinkage of deformed plastic was significantly reduced, as the SiC particles acted as a limitation to displacements, thereby increasing wear resistance. When SiC content is increased in the matrix, both WR and COF decreased [22].

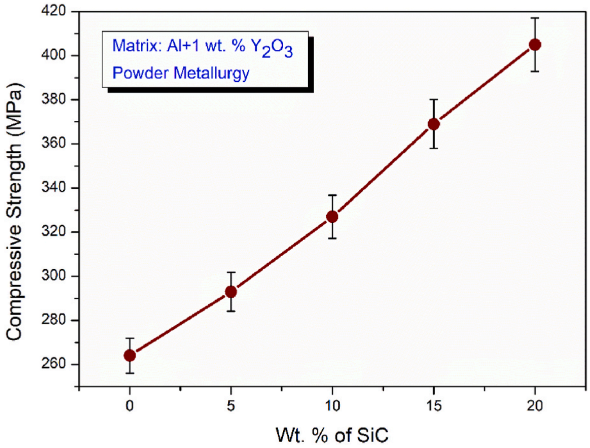

Fig. 8. 'CS' of Al + 1 wt%Y_2O_3 + SiC hybrid composites.

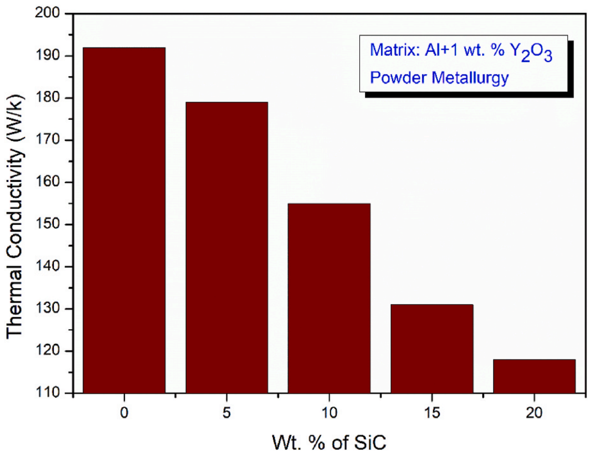

Fig. 9. Thermal conductivity of Al + 1 wt%Y_2O_3 + SiC hybrid composites.

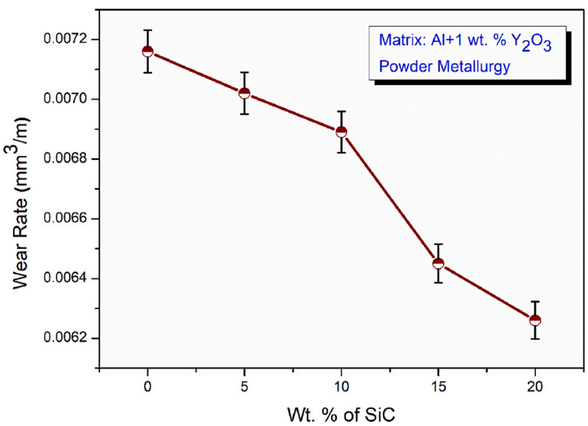

Fig. 10. Wear rate of Al + 1 wt%Y_2O_3 + SiC hybrid composites.

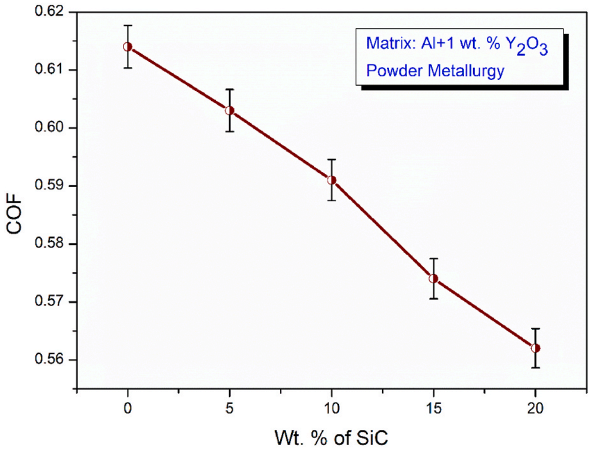

Fig. 11. COF of Al + 1 wt%Y_2O_3 + SiC hybrid composites.

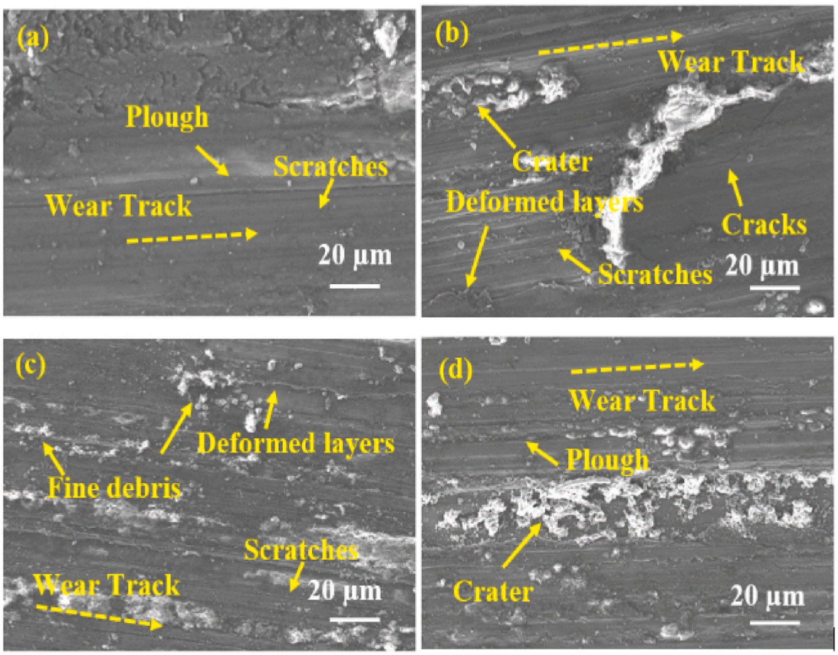

Fig. 12. (a)–(d) Worn surface morphology of the (a) Al + 1 wt% Y_2O_3 + 5 wt% SiC, (b) Al + 1 wt% Y_2O_3 + 10 wt% SiC, (c) Al + 1 wt% Y_2O_3 + 15 wt% SiC and (d) Al + 1 wt% Y_2O_3 + 20 wt% SiC composite samples.

4. Conclusion

Al + 1 wt% Y_2O_3 + SiC composites were produced by powder metallurgy route. From the result and discussions, the following conclusions were inferred.

- The chosen fabrication parameters ensured the consistent dispersal of Y_2O_3 and SiC particles in the Al − 1 wt% Y_2O_3 matrix.
- The density of the Al–Y_2O_3–SiC hybrid composites is increased while increasing the wt% of the SiC in the Al − 1 wt% Y_2O_3 matrix. Also, the porosity levels was found to be increased with increase in SiC content.
- The introduction of Y_2O_3 and increasing SiC percent increases both the hardness and CS of samples when compared to pure Al. SiC played a crucial part in strengthening the composite and the maximum CS was recorded as 405 MPa for the sample contain 20 wt% of SiC.
- With the inclusion of SiC and ytria reinforcements, K decreases from 192 to 118 W/k.
- The enrichment in wear resistance and lessening in COF values of Al–Y_2O_3–SiC hybrid composites was achieved due to the presence of hard SiC particles in the Al − 1 wt% Y_2O_3 matrix.

Author contribution statement

P.P. Shantharaman; V. Anandakrishnan; Sathish S; Ravichandran M; Naveenkumar R; Jayasathyakawin S; Rajesh S: Conceived and designed the experiments; Performed the experiments; Analyzed and interpreted the data; Contributed reagents, materials, analysis tools or data; Wrote the paper.

Data availability statement

No data was used for the research described in the article.

References

[1] S.C. Tjong, Recent progress in the development and properties of novel metal matrix nanocomposites reinforced with carbon nanotubes and graphene nanosheets, Mater. Sci. Eng. R. Rep. 74 (10) (2013) 281–350, https://doi.org/10.1016/j.mser.2013.08.001.

[2] Chen Fei, Nikhil Gupta, K. Behera Rakesh, K. Rohatgi Pradeep, Graphene-reinforced aluminum matrix composites: a review of synthesis methods and properties, JOM 70 (6) (2018) 837–845, https://doi.org/10.1007/s11837-018-2810-7.

[3] Afsaneh Dorri Moghadam, Emad Omrani, Pradeep L. Menezes, Pradeep K. Rohatgi, Mechanical and tribological properties of self-lubricating metal matrix nanocomposites reinforced by carbon nanotubes (CNTs) and graphene – a review, Compos. B Eng. 77 (2015) 402–420, https://doi.org/10.1016/j.compositesb.2015.03.014.

[4] S. Liu, M. Chen, X. Xiao, Influence of carbon content on aluminothermic reduction of ilmenite during hot pressing, JOM 71 (2019) 1822–1830, https://doi.org/10.1007/s11837-019-03428-5.

[5] A. Dey, K.M. Pandey, Wear behaviour of Mg alloys and their composites - a review, Int. J. Mater. Res. 109 (2018) 1050–1070, https://doi.org/10.3139/146.111707.

[6] S. Madhusudan, M.M.M. Sarcar, N.R.M.R. Bhargava, Fabrication and characterization of aluminium-copper composites, J. Alloys Compd. 471 (2009) 116–118, https://doi.org/10.1016/j.jallcom.2008.04.025.

[7] K. Soorya Prakash, P.M. Gopal, D. Anburose, V. Kavimani, Mechanical, corrosion and wear characteristics of powder metallurgy processed Ti-6Al-4V/B4C metal matrix composites, Ain Shams Eng. J. 9 (2018) 1489–1496, https://doi.org/10.1016/j.asej.2016.11.003.

[8] Chonghai Xu, Study on microstructure of alumina based rare earth ceramic composite, J. Rare Earths 24 (1) (2006) 217–221, https://doi.org/10.1016/S1002-0721(07)60364-0.

[9] V.A. Borodin, M Yu Starostin, T.N. Yalovets, Structure and related mechanical properties of shaped eutectic Al_20_3-$Zr0_2(Y_20_3)$ composites, J. Cryst. Growth 104 (1) (1990) 148–153, https://doi.org/10.1016/0022-0248(90)90324-E.

[10] Toshihiro Yamada, Ken Hirota, Osamu Yamaguchi, Mechanical properties of hot isostatically pressed zirconia (2 Mol% yltria)-reinforced Molybdenum disilicide composite, Mater. Res. Bull. 30 (7) (1995) 851–857, https://doi.org/10.1016/0025-5408(95)00073-9.

[11] R. Taherzadeh Mousavian, R. Azari Khosroshahi, S. Yazdani, D. Brabazon, A.F. Boostani, Fabrication of aluminum matrix composites reinforced with nano- to micrometer-sized SiC particles, Mater. Des. 89 (2016) 58–70, https://doi.org/10.1016/j.matdes.2015.09.130.

[12] J. Wang, Z. Li, G. Fan, H. Pan, Z. Chen, D. Zhang, Reinforcement with graphene nanosheets in aluminum matrix composites, Scripta Mater. 66 (2012) 594–597, https://doi.org/10.1016/j.scriptamat.2012.01.012.

[13] Akeem Damilola Akinwekomi, Microstructural characterisation and corrosion behaviour of microwave-sintered magnesium alloy AZ61/fly ash microspheres syntactic foams, Heliyon 5 (4) (2019), e01531, https://doi.org/10.1016/j.heliyon.2019.e01531.

[14] Navdeep Singh, Mir Irfan Ul Haq, Ankush Raina, Ankush Anand, Vinay Kumar, Sanjay Mohan Sharma, Synthesis and tribological investigation of Al-SiC based nano hybrid composite, Alex. Eng. J. 57 (3) (2018) 1323–1330, https://doi.org/10.1016/j.aej.2017.05.008.

[15] Reza Zare, Hasan Sharifi, Mohammad Reza Saeri, Morteza Tayebi, Investigating the effect of SiC particles on the physical and thermal properties of Al (6061)/SiCp composite, J. Alloys Compd. 801 (2019) 520–528, https://doi.org/10.1016/j.jallcom.2019.05.317.

[16] Negin Ashrafi, Azmah Hanim Mohamed Ariff, Masoud Sarraf, Shamsuddin Sulaiman, SaiHong Tang, Microstructural, thermal, electrical, and magnetic properties of optimized Fe_3O_4–SiC hybrid nano filler reinforced aluminium matrix composite, Mater. Chem. Phys. 258 (2021), 123895, https://doi.org/10.1016/j.matchemphys.2020.123895.

[17] Reza Zare, Hasan Sharifi, Mohammad Reza Saeri, Morteza Tayebi, Investigating the effect of SiC particles on the physical and thermal properties of Al (6061)/SiCp composite b, J. Alloys Compd. 801 (15 September) (2019) 520–528.

[18] J. Llorca, A. Needleman, S. Suresh, An analysis of the effects of matrix void growth on deformation and ductility in metal-ceramic composites, Acta Metall. Mater. 39 (10) (1991) 2317–2335, https://doi.org/10.1016/0956-7151(91)90014-R.

[19] K. Purazrang, P. Abachi, K.U. Kainer, Investigation of the mechanical behaviour of magnesium composites, Compos. A 25 (4) (1994) 296–302, https://doi.org/10.1016/0010-4361(94)90222-4.

[20] M. Penchal Reddy, R.A. Shakoor, Gururaj Parande, Vyasaraj Manakari, F. Ubaida, A.M.A. Mohamed, Manoj Gupta, Enhanced performance of nano-sized SiC reinforced Al metal matrix nanocomposites synthesized through microwave sintering and hot extrusion techniques, Prog. Nat. Sci. 27 (5) (2017) 606–614, https://doi.org/10.1016/j.pnsc.2017.08.015.

[21] E.A. Shalaby, A.Y. Churyumov, D.H. Besisa, A. Daoud, M.T. Abou El-khair, A comparative study of thermal conductivity and tribological behavior of squeeze cast A359/AlN and A359/SiC composites, J. Mater. Eng. Perform. 26 (7) (2017) 3079–3089, https://doi.org/10.1007/s11665-017-2734-3.

[22] H.O.U. Qingyu, Z. Huang, G.A.O. Jiasheng, Effects of Y2O3 on the microstructure and wear resistance of cobalt-based alloy coatings deposited by plasma transferred arc process, Rare Met. 26 (2) (2007) 103–109, https://doi.org/10.1016/S1001-0521(07)60168-5.

[23] X. Na, L. Wenqing, Z. Liu, T. Muthuramalingam, Effect of scandium in Al-Sc and Al-Sc-Zr alloys under precipitation strengthening mechanism at 3500C aging, Met. Mater. Int. 27 (12) (2021) 5145–5153, https://doi.org/10.1007/s12540-020-00844-0.